Combined Optical and Electronic Sensing of Epithelial Cells Using Planar Organic Transistors

*Marc Ramuz, Adel Hama, Miriam Huerta, Jonathan Rivnay, Pierre Leleux, and Róisín M. Owens**

In recent years, a push towards in vitro models for toxicology and drug development has arisen partly from the cost associated with animal models, but also from regulation that requires the reduction and replacement of animal experimentation. To date, the main focus has been on development of cellular models to replace animal studies where possible, using traditional cell-biology methods, such as fixed-cell imaging or quantification of biomolecules from dead cells. These methods are rarely amenable to high-throughput screening, are generally high-cost and usually require the use of labels such as chromophores and fluorophores. There is a definite need for the development of new technologies and materials for monitoring in vitro cell models.

One particularly promising whole-cell based system amenable to high-throughput and label-free testing forin vitro toxicology and drug screening, is electrical impedance sensing (or electrochemical impedance spectroscopy (EIS)), and a number of commercially available EIS-based systems are now on the market.[1] EIS is a technique which has long been used to determine mechanisms of reactions occurring at electrode/electrolyte interfaces.[2] EIS was first demonstrated for monitoring cell attachment and spreading on electrodes in the 1980s, first at fixed frequencies, but later by scanning a range of frequencies, and may simply be explained as measurement of changes in impedance due to the presence of cells on or near electrodes.[3–5] Initial work on electrical cell-substrate impedance sensing (ECIS) demonstrated that this technology could be used to determine such parameters as distance from the substrate,[6] cell adhesion and proliferation[4,7] and thus could be used in applications like wound healing,[8] and cell spreading.[9] Variations on this technology have also been developed by a number of different groups and have shown significant potential for medium to high-throughput monitoring of cells in vitro.[10–12] Two different formats exist in EIS-based devices; the first, the nonplanar format, involves cells that are grown on filters between the electrodes, whereas the second, the planar format, has cells grown directly on the electrodes. Although the filter format is compatible with transport assays used in drug development as it allows sampling from the lower compartment, it is very difficult to image cells on the filters.[10] Indeed, although all the variations on EIS demonstrate the potential of electronic monitoring for assessing cell integrity and function, in general these systems do not allow high-resolution imaging and are thus incompatible with microscopy systems used for life-sciences research, still recognized as the gold standard for monitoring cell health and function, particularly at the molecular level.[13] This highlights a particular drawback with electrical monitoring, which is the inability to unambiguously correlate a measured electrical signal, especially in non-electrogenic cells (where a passive electrical resistance is being measured rather than for example an action potential seen in electrogenic cells such as nerve cells), with an event occurring in the life cycle of the cell. Advances in time-lapse microscopy and availability of reagents that allow live–cell imaging have been made that allow for more relevant capturing of dynamic events occurring in the cell, hitherto impossible with static imaging techniques;[14] however, a number of disadvantages of optical monitoring technologies still remain, such as the use of costly chromo-/fluorophores, and labor intensive protocols. The ability to simultaneously monitor cells both optically and electrically in vitro is thus a very attractive proposition, with high enough resolution to not only relate electronic signals to events occurring in the cell, but also to exploit the complementarity of these techniques, to monitor events that may easily be captured electronically and not optically or *vice versa*.

We previously developed an organic electrochemical transistor (OECT) based on poly(3,4-ethylenedioxythiophene):poly(styrenesulfonate) (PEDOT:PSS), capable of monitoring the integrity of epithelial barrier tissue cells grown on filters, with unprecedented temporal resolution and high sensitivity.[15] This device has been validated against existing toxicology techniques[16,17] and has been transitioned towards more high-throughput systems capable of long-term operation under physiological conditions.[18] However, this device was originally configured as a non-planar transistor with a commercially available Transwell filter, and was therefore incompatible with high-resolution optical monitoring. Herein, we describe the development of a

Dr. M. Ramuz, A. Hama, Dr. M. Huerta, Dr. J. Rivnay, Dr. P. Leleux, Dr. R. M. Owens
Department of Bioelectronics
Ecole Nationale Supérieure des Mines CMP-EMSE, MOC
880 avenue de Mimet 13541, Gardanne, France
E-mail: owens@emse.fr

P. Leleux
Aix-Marseille Université
Institut de Neurosciences des Systèmes
13005, Marseille, France

P. Leleux
Inserm, UMR_S 1106
13005, Marseille, France

P. Leleux
Microvitae Technologies, Pôle d'Activité Y. Morandat
13120, Gardanne, France

DOI: 10.1002/adma.201401706

ADVANCED MATERIALS
www.advmat.de

www.MaterialsViews.com

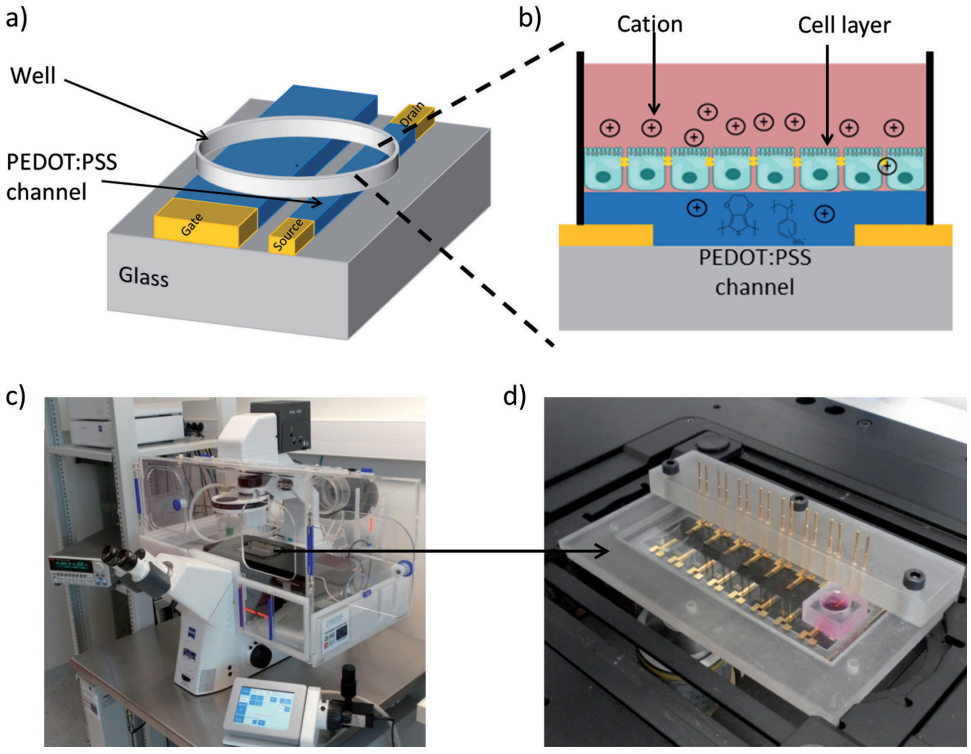

Figure 1. Simultaneous optical and electronic recording. a,b) Schematic of device which consists of a PEDOT:PSS channel and gate patterned onto a glass slide. Cells and media were contained inside a 3D-printed/PDMS well. Under applied gate voltage, cations from the media penetrate through the cell layer and de-dope the channel. c) Photograph of the optical microscope equipped for long-term live-cell culture. d) 8 OECTs connected via a 3D-printed holder adjusted for the microscope, pictured here on the microscope stage. Connections are made by spring-loaded contacts.

planar all-polymer transistor based on the conducting polymer PEDOT:PSS, compatible with low-cost production techniques such as ink-jet printing, or roll-to roll processing. Further, we take advantage of the optical transparency of PEDOT:PSS to demonstrate simultaneous electronic and optical monitoring of epithelial cells in vitro, with acquisition of high-resolution time-lapse images. We highlight the complementarity of these techniques, illustrating the advantage of electronic monitoring over optical monitoring in certain cases, and finally, demonstrate an acute example of how these complementary techniques lead us from the observation of an electronic signal in sub-confluent (before the cells have completely covered the surface) epithelial cell monolayers, to investigate the formation of structures important for ion-regulation in these cell types.

The planar OECT used for these studies is illustrated in **Figure 1**. In the current configuration both the channel and the gate consists of PEDOT:PSS, although gold was used as a contact material (Figure 1a). Wells were either 3D printed or made of polydimethylsiloxane (PDMS) and affixed to the device for cell growth. The mechanism of the OECT for monitoring barrier tissue integrity has been described previously;[15] however, in the previous case the barrier tissue cells were grown on a filter positioned between a top Ag/AgCl gate and the channel consisting of PEDOT:PSS. In the current device, barrier tissue cells were seeded directly into a well on top of the planar device. The well was designed to cover not only a section of the channel but also a section of the gate (Figure 1a). Upon application of a positive gate voltage (V_{GS} = 0.3V), the cell monolayer covering the channel reduces the flux of cations from the media to the channel. This restriction of cation flow results in slower de-doping of the channel and thus a modification of the channel current (Figure 1b).[15] In contrast to the previous configuration, the gate is now located below the cell monolayer. In agreement with previous studies using ECIS, we hypothesize that due to the high resistance of the nanometer-sized electrolyte filled cleft between the cells and the substrate, the gate current passes through the cell monolayer into the medium and then back through the cell monolayer into the channel, rather than laterally between the gate and channel.[19] In the present system, eight OECTs were fabricated on a single glass slide to allow for simultaneous measurements of multiple devices. The glass slide is positioned inside a 3D-printed holder with spring-loaded contact pins for connections (Figure 1d). This holder is in turn placed on a microscope stage (Figure 1c). The microscope is equipped with a sealed chamber to mimic the conditions found inside a cell culture incubator.

Taking advantage of the optical transparency of the PEDOT:PSS film, high-resolution images of the cells can be recorded. PEDOT:PSS has an extinction coefficient below 0.3 in the visible range[20] (for comparison, the extinction coefficient of gold is between 2 and 5 in the visible range depending on the wavelength.[21] In contrast to existing technologies, high-resolution images can easily be produced in bright field or fluorescence (see work by Strakosas et al.[22] and Figure S1 in the Supporting Information for representative images). In contrast, imaging on gold electrodes requires the use of an upright microscope with a long distance objective, due to the inefficient

transmission of the low intensity fluorescence signal through the gold layer.[23] We recorded the electrical characteristics of the cell monolayer using the OECT device (under physiological conditions), while simultaneously collecting optical images in time-lapse mode. This technique allows precise correlation between the function of the cell monolayer (electrical characteristics) and the morphology of the cells (optical characteristics).

Madin Darby Canine Kidney (MDCK-I) cells are a well characterized cell-line which has been shown to develop properties of transporting epithelia when they grow on membranes[24] and on solid supports.[25] Using a more-traditional chopstick electrode set-up, MDCK-I cells have been shown to reach resistances of ca. 1000 Ω cm^2 as early as 4–5 days after seeding.[26] In the case of the OECT, there is no direct measurement of the ion conductance (or resistance) across the cell monolayer. Rather, the current through the OECT channel is linearly proportional to the number of ions that have entered the channel, which in turn determines the speed at which the transistor reaches steady state.[27] The time constant, τ, is used as a figure of merit for the electrical characterization of the ion flow through epithelia as measured by the OECT. Extended information on determination of τ has been reported previously.[18] For electrical characterization of MDCK-I cells seeded onto the OECT, the channel current was measured upon application of a positive square-pulse gate voltage. Similar to the charge and discharge of a capacitor in an RC electronic circuit, the channel current can be fit by an exponential equation (see materials and methods) and the τ value extracted as a fit parameter. The data is then normalized between 0 and 1, where 1 is the highest τ value obtained (corresponding to the lowest amount of ion flux across a functional cell monolayer), and 0 is the lowest value τ obtained (corresponding to a device with no cells). After seeding of the MDCK-I cells, the rise of τ (**Figure 2**a) started as early as 6 h and plateaued between 35–50 h. Within this time frame, optical images of the cell monolayer (Figure 2b) showed the development of a regular, confluent monolayer on the device. Subsequently, the τ value decreased to 0 at approcimately 95 h, where correlation of the signal with the optical images (see the Supporting Information for a video) shows that many of the cells are in suspension and no longer attached to the substrate. This is anticipated since the media remains unchanged throughout the duration of the experiment. A very noticeable and, to our knowledge, previously unknown phenomenon was the onset of an increase of τ before the cells had completely covered the surface (were sub-confluent). Indeed, as seen in Figure 2b, the full coverage of MDCK-I cells on the channel occurred after t = 18 h, corresponding to a normalized τ of approximately 0.5. These data suggest that the structures which regulate ion flow in epithelial cells are functional before the cell monolayer is confluent.

The exact sequence of events that occur in the development of the structures that regulate ion flow in epithelia after the initial contact formed between adjacent cells remains unknown.[28] The formation of junctions between cells is a highly regulated process; in epithelial cells, neighboring cells are known to form tight contacts, necessary for tissue formation. It is thought that spot-like adhesions form first, at the tip of the initial cell-cell contacts, which then develop into belt-like adherens junctions (AJ),[29,30] followed by formation of tight junctions (TJ) at the apical side of the AJ.[31] These TJs have a barrier function to selectively limit the flow of ions and macromolecules. ZO-1 is a cytoplasmic actin binding protein that plays an important role in both the AJ and the TJ, being present with E-cadherin in the AJ and then segregating to co-localize with other proteins such as Occludin and Claudin-1 in the TJ.[32–34] To study TJ function, cells are usually seeded at high concentrations, and their resistance is measured at designated time points post confluence, which may be a matter of hours if the density is high enough for the cells to cover a surface without dividing.[35,36] In the typical Transwell filter set-up, measurement of paracellular resistance is only possible post-confluency, as otherwise the gaps between groups of cells provide easy pathways for ion flux. In contrast, in a planar configuration made possible using the device reported here, it is possible to measure resistance to ion-flow before the cell monolayer becomes confluent since the cells are grown directly on the active area of the device. Reports using the ECIS device appear to indicate that a 'fully established cell matrix is required before the formation of tight junctions', however this is difficult to establish without recourse to simultaneous optical and electronic monitoring.[19] Our data clearly show that although this may be true locally (in isolated clusters of cells), functional TJs can form before confluence. To further investigate the origin of the electrical signal observed with the OECT, MDCK-I cells were seeded at low densities to achieve incomplete coverage (quantification of sample coverage is shown in Figure S2 in the Supporting Information: 2% at day 1, 21% at day 3 and 100% at day 5). Representative immunofluorescence images from cells stained for ZO-1, Claudin-1, Occludin and E-cadherin at days 1, 3 and 5 post seeding, are shown in Figure 2c. As expected, E-cadherin is present at cell-cell contacts from day 1, and, although there is also some cytoplasmic staining, it is absent at the leading or outside edges of the cells. By day 5, E-cadherin appears only at the cell periphery. A similar pattern is seen for the TJ proteins Occludin, Claudin-1 and ZO-1, although the disappearance of the cytoplasmic fraction appears to be most rapid for ZO-1, where no cytoplasmic staining is visible at day 3, followed by Occludin and then Claudin-1. Together with the electrical monitoring data, we believe this provides clear evidence that ion flow is regulated as soon as the key tight TJ proteins are present between adjacent cells, and does not depend on a confluent monolayer of cells to begin regulating ion flow. This does not preclude that the function of the TJ may evolve post-confluence, and indeed TER measurements are often seen to peak before stabilizing, possibly indicating a balance between 'tight' and 'leaky' claudin expression.[37,38]

The majority of work in the literature on electrical measurements of non-electrogenic cells grown on surfaces comes from ECIS measurements, which determines the impedance of cell monolayers grown on electrodes, and can correlate the signal at different frequencies to a variety of cell parameters by modelling the different elements in an equivalent circuit.[3,7] The most basic information from ECIS is related to the coverage of cells on the electrodes which results in changes in impedance.[9] One possibility for the increase in τ observed during growth of MDCK-I cells on the planar OECT, is that the signal is due to coverage of the cells on the surface of the device which could modify the ionic resistance and change the surface

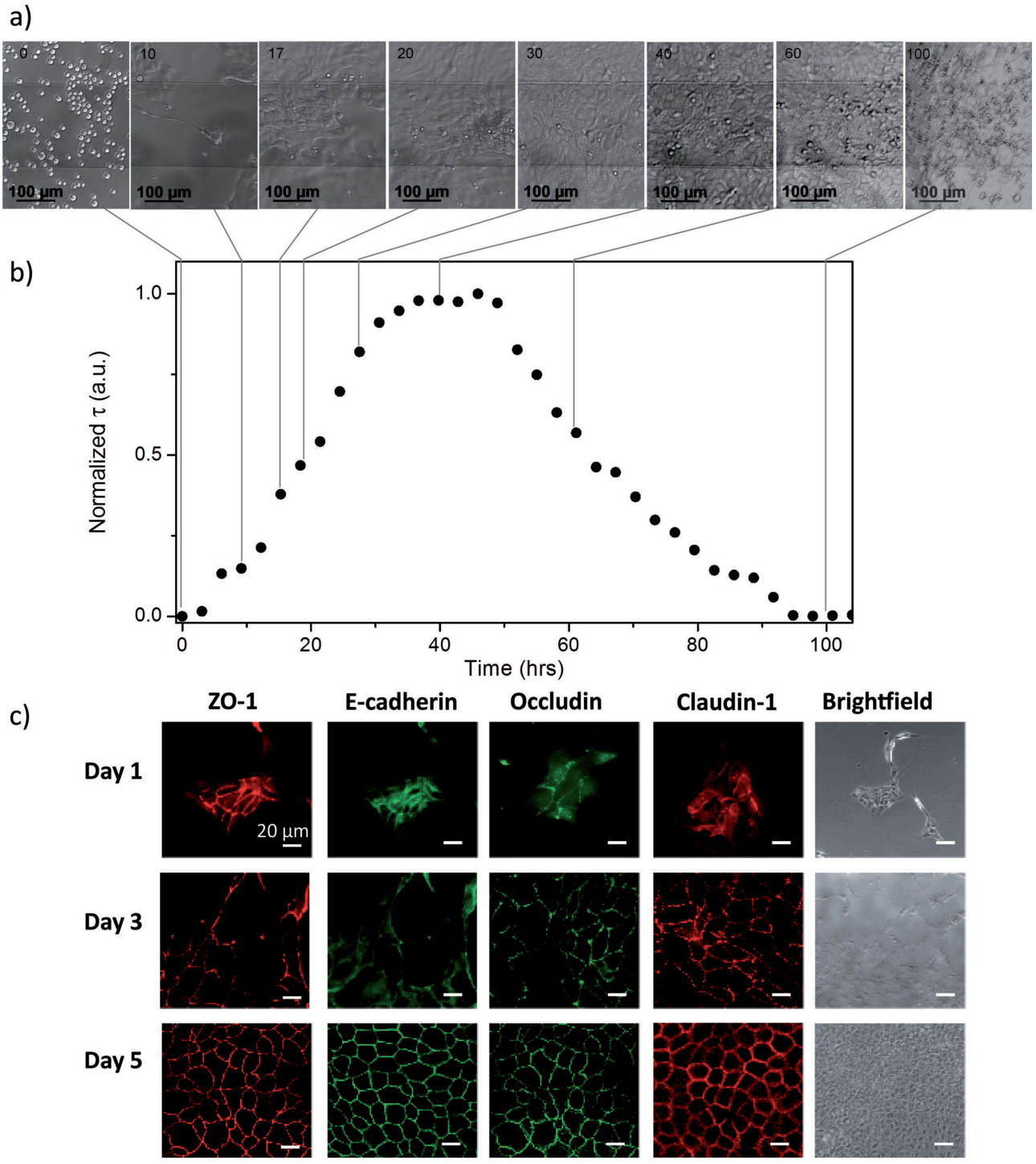

Figure 2. Electrical and optical characterization of MDCK-I cells on the planar OECT. MDCK-I were seeded at 10^5 cells / cm^2 and monitored for 4.5 days. a) Micro-optical images of MDCK-I on top of the channel area. The darker horizontal line in the middle of the picture corresponds to the PEDOT:PSS channel. b) Electrical characteristics with a measurement taken every 3 h. c) Immunofluorescence images taken on sub-confluent MDCK-I monolayers show presence of ZO-1 and E-cadherin at the cell periphery very early on. Occludin and Claudin-1 localize in the cytoplasm and just in the cell contacts the first 3 days. At day 5 all the proteins are present at the cell borders.

capacitance due to the adhesion of the cells on PEDOT:PSS. To test whether the changes in τ measured by the OECT upon growth of the cells on the device are attributable to the barrier function of the cells, or simply to a coverage effect, different types of epithelial cells were seeded onto devices and allowed to grow to confluence and beyond. As before, the OECT was used to monitor the electrical behavior of the cells, with simultaneous optical monitoring using the microscope. Three different

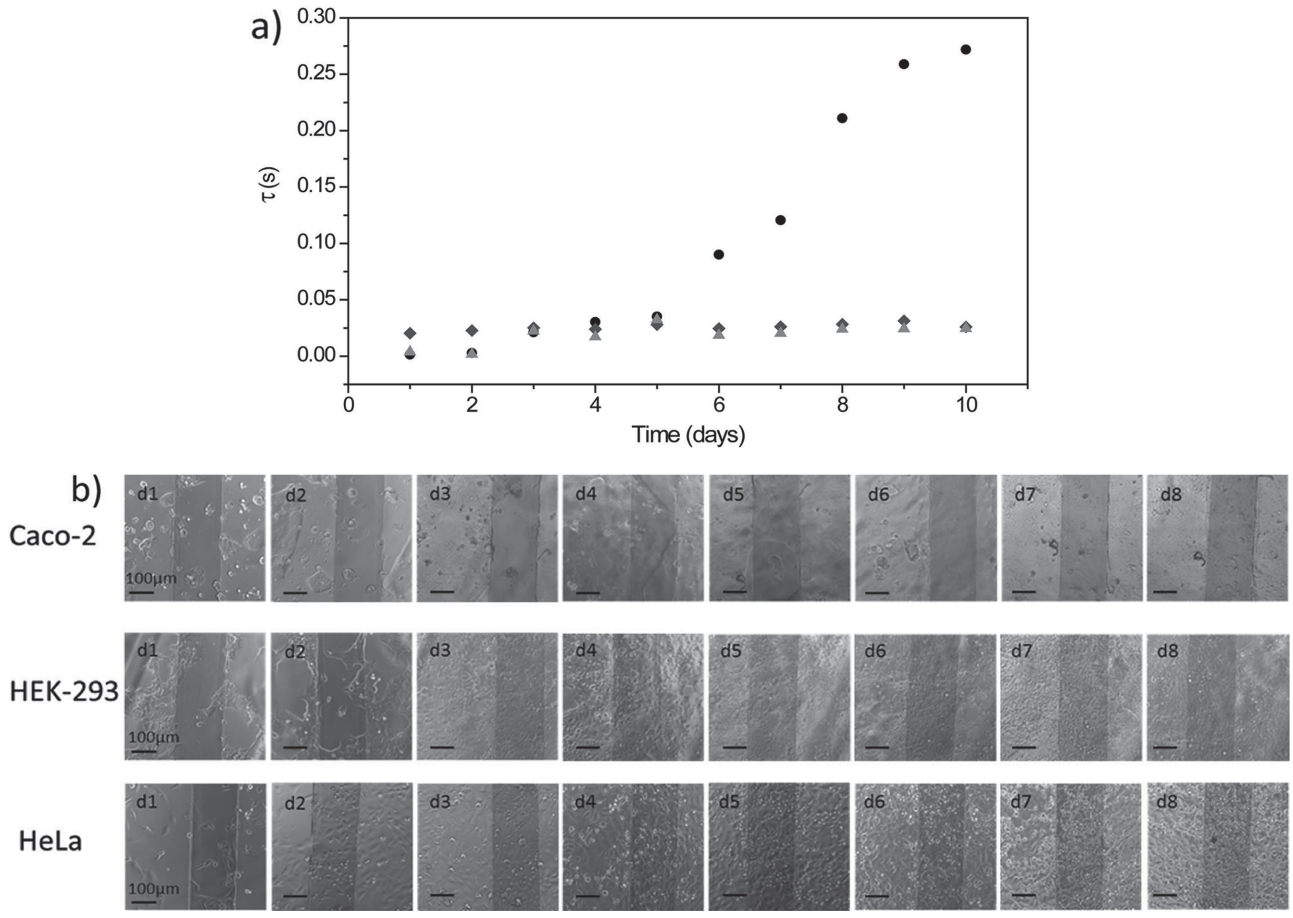

Figure 3. Electrical signal measured by OECT is related to barrier function of cells. a) Electrical characteristics of various cell lines measured over 8 days: dark round markers for Caco-2 cells, dark-grey diamonds markers for HEK-293 cells, and grey triangle markers for HeLa cells. b) Corresponding micro-optical images of cell coverage over the channel area.

cell lines were compared, Caco-2 cells (a human colon-cancer epithelial cell-line), HEK-293 cells (human embryonic kidney epithelial cells) and HeLa cells (a human cervical-cancer epithelial cell-line). Neither HeLa nor HEK-293 have ever, to our knowledge, been reported to have a measurable TER. HEK-293 cells have been reported to have no expression of Claudins 1–5, nor any evidence of TJ strands.[39] Caco-2 cells are known to differentiate and form TJs; however they require approximately 3 weeks to generate a stable TER of ca. 400 Ω cm^2 on Transwell filters.[17]

It is clear from **Figure 3**a that neither HEK-293 cells nor HeLa cells show a significant increase in the τ value regardless of the surface coverage. HEK-293 cells show complete, even coverage of cells on the device by day 3, however there is no change in the τ value. The same is true for HeLa cells, although the cell monolayer is not as regular as with the HEK-293 cells, and some gaps are visible between cells. For Caco-2 cells, the τ value does not change significantly for the first 5 days. At day 6 however, there is a noticeable upward trend until the end of the experiment at day 8. This is consistent with the behavior observed when these cells are grown on Transwell filters, reaching average TER values of 100 Ω cm^2 after 5 days, and 300 Ω cm^2 after 10 days.[17] An interesting corollary from this experiment is that Caco-2 cells can differentiate with respect to their TJ function even on a solid support, without the cues that can be provided from below thanks to a permeable membrane such as the Transwell filter, something that had previously been shown for MDCK-I cells.[25]

As a further test of whether the changes in τ measured by the OECT upon growth of the cells on the device are attributable simply to coverage of the cells on the surface or could be ascribed to blocking of ions by TJs, we used EGTA (ethylene glycol tetraacetic acid), a specific Ca^{2+} chelator which is known to compromise the integrity of TJs and result in a rapid decrease in the resistance of epithelia to ion flow.[16,24]

Figure 4a shows the electrical measurement of an MDCK-I monolayer after addition of varying concentrations of EGTA. At low concentrations of EGTA (1 mM), there was no reduction of τ and thus the resistance to ion flow was still intact. Since the concentration of Ca^{2+} in media is usually 1–2 mM, there may still be enough Ca^{2+} present for the barrier function to be maintained. However, for concentrations of 5 mM, 10 mM and 100 mM EGTA, the barrier function of the cells is seen to decrease rapidly, reaching a normalized value of 0 within 10 min at 100 mM EGTA. In contrast, the corresponding optical images (Figure 4b) show no visible change in the cell monolayer, regardless of the concentration of EGTA. Even after 14 min of 100 mM EGTA treatment the cell monolayer looks completely unchanged and confluent on the device. We

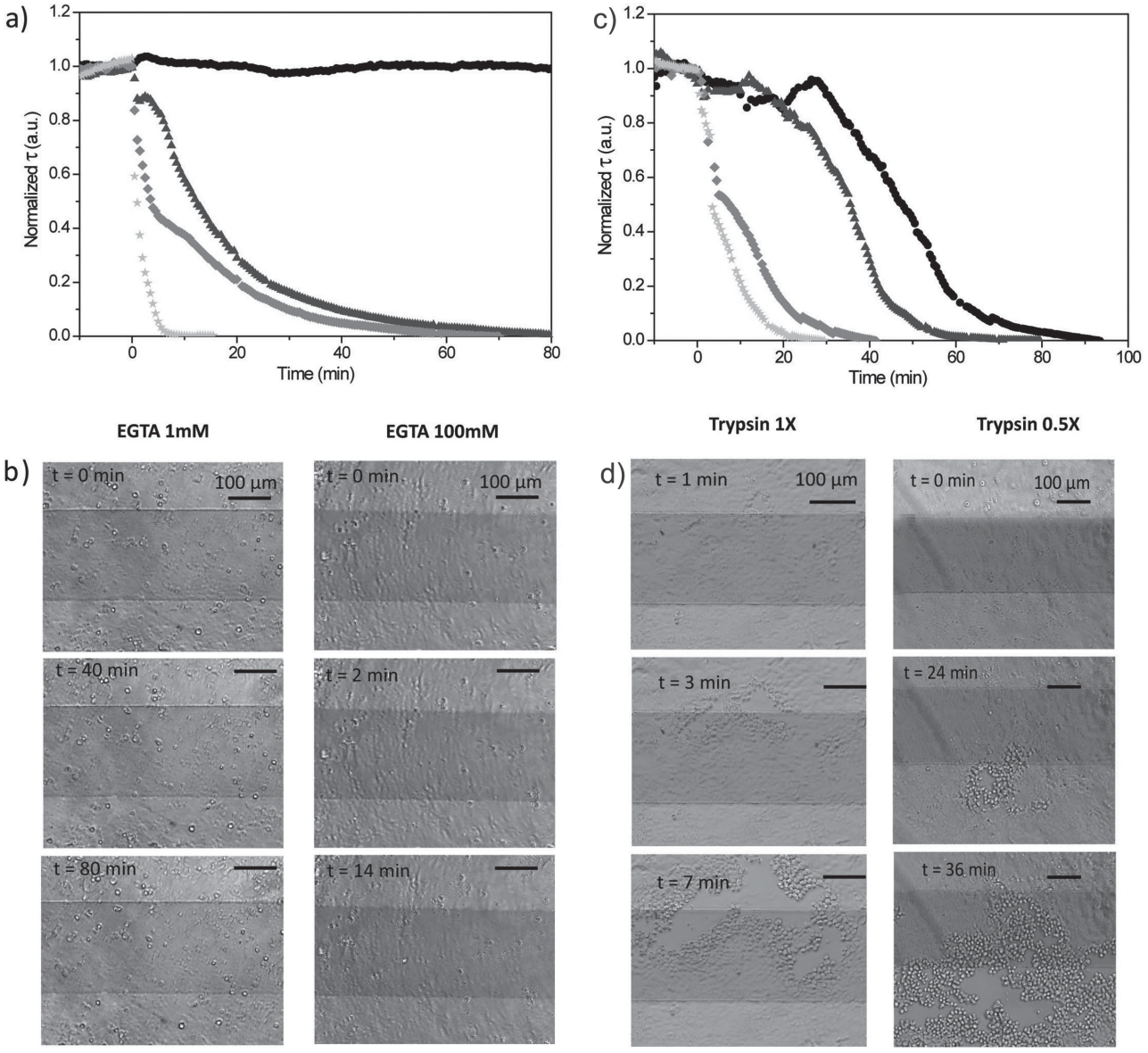

Figure 4. Effect of EGTA and trypsin-EDTA on MDCK-I barrier function. a) Electrical characteristics of MDCK-I barrier tissue measured by an OECT. Normalized τ value of 1 corresponds to an intact cell monolayer and 0 to a disrupted one. At t = 0 min, EGTA was added according to the following concentrations: 1 mM for dark round markers, 5 mM for dark-grey triangle markers, 10 mM for grey diamond markers, and 100 mM for light-grey star markers. b) Corresponding micro-optical images for EGTA = 100 mM and EGTA = 1 mM. c,d) Effect of Trypsin-EDTA on MDCK-I barrier: c) Electrical characteristics of MDCK-I monolayers measured by an OECT. Normalized τ of 1 corresponds to an intact cell monolayer and 0 to a disrupted one. At t = 0 min, Trypsin-EDTA was added according to the following concentrations: 0.25X for dark round markers, 0.5X for dark-grey triangle markers, 0.75X for grey diamond markers, and 1X for light-grey star markers. d) Corresponding micro-optical images for trypsin-EDTA 0.5X and 1X.

conclude thus that the normalized τ value is attributable to the barrier function of the cells, and not simply to growth/coverage of the cells on the device (see the Supporting Information for videos of the data shown here).

The integrin proteins, which are the major cell-substrate binding proteins, are known to be dependent on Mg^{2+} and therefore the addition of EGTA is unlikely to affect substrate binding.[40] The addition of trypsin-EDTA however, is known to detach cells from surfaces. Trypsin is a protease that is routinely used to detach cells from surfaces, by non-specifically cleaving proteins (at lysine or arginine residues), while EDTA chelates metal ions such as Ca^{2+} and Mg^{2+}. As shown in Figure 4c, after trypsin-EDTA treatment the barrier function of the MDCK-I cells decreases rapidly, with the time required for complete removal of the barrier properties decreasing with increasing trypsin-EDTA concentration. In contrast to the EGTA treatment, the addition of trypsin-EDTA results in a detachment of the cell monolayer, clearly visible from the optical images (Figure 4d). Additionally, the destruction of the barrier function of the cells precedes the detachment of the cell monolayer; at 1X trypsin-EDTA, the first gap in the cell monolayer is visible at 3 min, corresponding to a decrease in the

normalized τ value of 25%, whereas the decrease in electrical signal clearly begins in under a minute.

The OECT is a versatile, robust, low-cost and fully transparent device which can be used to record barrier tissue properties. The ability to simultaneously record electrical and optical characteristics is greatly beneficial for monitoring the integrity of *in vitro* models of cells. In this report, we show evidence of one situation in which the combined electronic and optical information provide new information on the growth and behavior of cells in culture: notably we have demonstrated that the formation of TJs in MDCK-I cell layer occurs before full confluence of the cells. This observation is made possible in the device shown here which allows continuous measurements of ion flow in epithelial cells pre- and post-confluency coupled with image capture of cell coverage at high resolution. We clearly show that the measured electrical signal is due to TJ-related barrier tissue formation rather than simple cell coverage; the presence of cells on the active area of the OECT does not modify the transistor response to gate pulse voltage unless the cells present barrier properties. Measurement of barrier properties by OECTs is a rapid, and potentially low-cost method and thus represents real future potential as a new technology for high-throughput dynamic monitoring of live-cell toxicology.

Experimental Section

OECT Fabrication: The conducting polymer formulation consisted of PEDOT:PSS (Heraeus, Clevios PH 1000), with ethylene glycol (Sigma–Aldrich, 0.25 mL for 1 mL PEDOT:PSS solution), 4,dodecylbenzenesulfonic acid (DBSA) (0.5 µL/mL), and 3-glycidoxypropyltrimethoxysilane (GOPS) (10 mg/mL). On a clean glass substrate (75 mm × 25 mm), gold source and drain contacts were patterned via photolithography, thermal evaporation, and subsequent lift-off. Photoresist S1813 (MicroChem Corp.) was spin-coated at 3000 rpm for 30 s on the glass substrate. Patterns were defined by photolithography (Chrome mask and Mask Aligner). MF-26A was used as developer. Then, 5 nm and 100 nm of chromium and gold respectively, were evaporated. Finally, the photoresist was lifted-off in an acetone bath under sonication for 1 h, which left the substrate with the source and drain Au contacts only. PEDOT:PSS channel dimensions were patterned using a parylene peel-off technique described previously,[41] resulting in a PEDOT:PSS channel with width and length of 200 µm and 4 mm, respectively, and thickness of 460 nm. The PEDOT:PSS gate was 1 mm width and 4 mm length. Following PEDOT:PSS deposition, devices were baked for 1 h at 140 °C under atmospheric conditions. Either 3D printed or PDMS wells of 0.5 cm^2 (hole diameter of 0.8 cm) defined the cell-growth area.

OECT Operation: All measurements were done using the PEDOT:PSS film as gate electrode and cell media (as described below) as the electrolyte. Experiments were performed in an XL multi SI humidified incubator from PECON GmbH mounted on a microscope Axio Observer Z1 from Carl Zeiss MicroImaging GmbH. The temperature and CO_2 level were at 37 °C and 5%, respectively. The measurement parameters were chosen to avoid exposing the cell monolayers to a voltage drop above 0.5 V, as high voltages have been shown to damage bilayer membranes.[42] The recording of the OECTs was performed using a Keithley 2612 Source Meter and customized Labview software. OECT data were collected using the following parameters: $V_{DS} = -0.2$ V, $V_{GS} = 0.3$ V, V_{GS} on time = 2 s, off time = 28 s.

Data Analysis: Data analysis was performed using a customized Matlab program to isolate and fit the time constant for each pulse as described previously.[18] In Figure 2 and 4, the data are then normalized using the following equation: $NR = (\tau_{no\ cells} - \tau)/(\tau_{no\ cells} - \tau_{cells})$, where τ_{cells} refers to the tau value in response to the application of the gate voltage of a barrier forming monolayer, and $\tau_{no\ cells}$ refers to the tau value in response to the application of the gate voltage of no barrier, with the dataset subsequently normalized to [0,1] scale, where 1 corresponds to intact cell monolayer and 0 to a disrupted one or absence of barrier monolayer.

Cell Culture: MDCK-I cells, Caco-2 cells, and HeLa cells were obtained from HPA culture collection. Cells were routinely maintained at 37 °C in a humidified atmosphere of 5% CO_2, in Dulbecco's modified Eagle mediumDMEM) low glucose (Advanced DMEM Reduced Serum Medium 1X, Invitrogen) with 2 mM Glutamine (Glutamax-1, Invitrogen), 10% fetal bovine serum (FBS) (Invitrogen), 0.5% PenStrep (PenStrep 100X, Invitrogen) and 0.1% Gentamicin (Gentamicin 100X, Invitrogen). HEK-293 cells were a kind gift from Marc Borsotto (IPMC, Valbonne).

EGTA and Trypsin-EDTA Experiments. MDCK-I cells were grown directly on top of the OECT. They were maintained inside the incubator for 4 days until full confluence. Then, the substrate bearing the OECTs seeded with cells was placed onto the stage of the microscope. After 1 h required for stabilization, the recording of the electrical signal of the OECT and time-lapse optical recording was started. After approximately 15 min and while continuing the recording, the desired concentration of trypsin-EDTA or EGTA was added inside the well, which corresponds to time $t = 0$ min in Figure 4. Note that trypsin-EDTA 1X corresponds to 0.05% of trypsin with 0.02% EDTA.

Immunofluorescence: Cells were washed three times with cold PBS 1X (Ca^{2+}/Mg^{2+}) pH 7.4, then fixed and permeabilized with a mix of 4% paraformaldehyde, 0.1% Triton X-100 during 3 min at 4 °C. Cells were then incubated with 4% paraformaldehyde for 15 min at 4 °C, then washed with cold PBS 1X (Ca^{2+}/Mg^{2+}) pH 7.4 and incubated in blocking solution (3% bovine serum albumin (BSA), 0.3 M Glycine) for 1 h at room temperature. This was followed by addition of primary antibodies, rabbit anti-ZO-1, rabbit anti-Claudin-1, mouse anti-E-cadherin, mouse anti-Occludin (Invitrogen) in blocking solution for 1 h at 37 °C. They were washed three times with cold PBS 1X (Ca^{2+}/Mg^{2+}) pH 7.4 and incubated with the secondary antibodies Alexa Fluor 488 donkey anti-mouse and Alexa Fluor 568 donkey anti-rabbit (Molecular Probes) for 1 h at 37 °C. Finally, the cells were incubated for 5 min at room temperature with Fluoroshield with DAPI (Sigma–Aldrich), mounted, and examined using a fluorescence microscope.

Supporting Information

Supporting Information is available from the Wiley Online Library or from the author.

Acknowledgements

The authors gratefully acknowledge funding from the European Research Council ERC-2010-StG. Proposal No 258966 (IONOSENSE), as well as a Marie Curie Fellowship (JR).

Received: April 15, 2014
Revised: July 28, 2014
Published online: September 1, 2014

[1] C. W. Scott, M. F. Peters, *Drug Discovery Today* **2010**, *15*, 704.
[2] F. Alexander, D. Price, S. Bhansali, *IEEE Rev. Biomed. Eng.* **2012**, DOI: 10.1109/rbme.2012.2222023.
[3] I. Giaever, C. R. Keese, *Proc. Natl. Acad. Sci. USA* **1984**, *81*, 3761.
[4] I. Giaever, C. R. Keese, *Nature* **1993**, *366*, 591.
[5] I. Giaever, C. R. Keese, *Proc. Natl. Acad. Sci. USA* **1991**, *88*, 7896.

[6] C. R. Keese, J. Wegener, L. Giaever, *Genet. Eng. News* **2005**, *25*, 42.
[7] P. Mitra, C. R. Keese, I. Giaever, *BioTechniques* **1991**, *11*, 504.
[8] C. R. Keese, J. Wegener, S. R. Walker, I. Giaever, *Proc. Natl. Acad. Sci. USA* **2004**, *101*, 1554.
[9] J. Wegener, C. R. Keese, I. Giaever, *Exp. Cell Res.* **2000**, *259*, 158.
[10] J. Wegener, D. Abrams, W. Willenbrink, H. J. Galla, A. Janshoff, *BioTechniques* **2004**, *37*, 590.
[11] C. Xiao, J. H. Luong, *Toxicol. Appl. Pharmacol.* **2005**, *206*, 102.
[12] K. Benson, S. Cramer, H.-J. Galla, *Fluids Barriers CNS* **2013**, *10*, 5.
[13] B. F. De Blasio, M. Laane, T. Walmann, I. Giaever, *BioTechniques* **2004**, *36*, 650.
[14] D. L. Coutu, T. Schroeder, *J. Cell Sci.* **2013**, *126*, 3805.
[15] L. H. Jimison, S. A. Tria, D. Khodagholy, M. Gurfinkel, E. Lanzarini, A. Hama, G. G. Malliaras, R. M. Owens, *Adv. Mater.* **2012**, *24*, 5919.
[16] S. Tria, L. Jimison, A. Hama, M. Bongo, R. Owens, *Biosensors* **2013**, *3*, 44.
[17] S. A. Tria, L. H. Jimison, A. Hama, M. Bongo, R. M. Owens, *Biochim. Biophys. Acta* **2013**, *1830*, 4381.
[18] S. A. Tria, M. Ramuz, M. Huerta, P. Leleux, J. Rivnay, L. H. Jimison, A. Hama, G. G. Malliaras, R. M. Owens, *Adv. Healthcare Mater.* **2014**, DOI: 10.1002/adhm.201300632.
[19] J. Wegener, Impedance Analysis of Cell Junctions, in *Nanotechnology, Part 6: Nanoprobes*, (Ed: H. Fuchs), Wiley-VCH, Weinheim, Germany **2010**, pp. 325–357.
[20] J. Gasiorowski, R. Menon, K. Hingerl, M. Dachev, N. S. Sariciftci, *Thin Solid Films* **2013**, *536*, 211.
[21] E. F. Schubert, Refractive index and extinction coefficient of materials, 2004, http://homepages.rpi.edu/~schubert/Educational-resources/Materials-Refractive-index-and-extinction-coefficient.pdf, accessed: **August 2014**.
[22] X. Strakosas, M. Sessolo, A. Hama, J. Rivnay, E. Stavrinidou, G. G. Malliaras, R. M. Owens, *J. Mater. Chem. B* **2014**, DOI: 10.1039/c3tb21491e.
[23] J. Wegener, Applied Biophysics publications, 2009, http://www.biophysics.com/publications/ECIS_Microscopy_V2_DINA4.pdf, accessed: **August 2014**.
[24] M. Cereijido, E. Robbins, W. Dolan, C. Rotunno, D. Sabatini, *J. Cell Biol.* **1978**, *77*, 853.
[25] C. M. Lo, C. R. Keese, I. Giaever, *Biophys. J.* **1995**, *69*, 2800.
[26] B. B. Finlay, B. Gumbiner, S. Falkow, *J. Cell Biol.* **1988**, *107*, 221.
[27] D. A. Bernards, G. G. Malliaras, *Adv. Funct. Mater.* **2007**, *17*, 3538.
[28] J. L. Maiers, X. Peng, A. S. Fanning, K. A. DeMali, *J. Cell Sci.* **2013**, *126*, 3904.
[29] J. Miyoshi, Y. Takai, *Adv. Drug Delivery Rev.* **2005**, *57*, 815.
[30] Y. Takai, H. Nakanishi, *J. Cell Sci.* **2003**, *116*, 17.
[31] R. Yamamura, N. Nishimura, H. Nakatsuji, S. Arase, T. Sasaki, *Mol. Biol. Cell* **2008**, *19*, 971.
[32] M. Itoh, A. Nagafuchi, S. Yonemura, T. Kitaniyasuda, S. Tsukita, S. Tsukita, *J. Cell Biol.* **1993**, *121*, 491.
[33] M. Furuse, M. Itoh, T. Hirase, A. Nagafuchi, S. Yonemura, S. Tsukita, S. Tsukita, *J. Cell Biol.* **1994**, *127*, 1617.
[34] M. Itoh, M. Furuse, K. Morita, K. Kubota, M. Saitou, S. Tsukita, *J. Cell Biol.* **1999**, *147*, 1351.
[35] K. J. Roux, S. A. Amici, B. S. Fletcher, L. Notterpek, *Mol. Biol. Cell* **2005**, *16*, 1142.
[36] M. S. Balda, L. Gonzalezmariscal, R. G. Contreras, M. Maciassilva, M. E. Torresmarquez, J. A. G. Sainz, M. Cereijido, *J. Membrane Biol.* **1991**, *122*, 193.
[37] B. Rothen-Rutishauser, S. D. Kramer, A. Braun, M. Gunthert, H. Wunderli-Allenspach, *Pharmaceuti. Res.* **1998**, *15*, 964.
[38] D. Gunzel, A. S. Yu, *Physiol. Rev.* **2013**, *93*, 525.
[39] J. Piontek, L. Winkler, H. Wolburg, S. L. Müller, N. Zuleger, C. Piehl, B. Wiesner, G. Krause, I. E. Blasig, *FASEB J.* **2008**, *22*, 146.
[40] E. F. Plow, T. A. Haas, L. Zhang, J. Loftus, J. W. Smith, *J. Biol. Chem.* **2000**, *275*, 21785.
[41] D. Khodagholy, M. Gurfinkel, E. Stavrinidou, P. Leleux, T. Herve, S. Sanaur, G. G. Malliaras, *Appl. Phys. Lett.* **2011**, *99*, 163304.
[42] D. A. Bernards, G. G. Malliaras, G. E. S. Toombes, S. M. Gruner, *Appl. Phys. Lett.* **2006**, *89*, 05305.